

Розроблено вдосконалену схему процесу електродугової металізації. Вона дозволяє врахувати плавлення оболонки і прилеглої порошкового стержня за рахунок обмеженої дії розпилюючого струменя безпосередньо на «внутрішню» поверхню торців електродів. Цей ефект забезпечує можливість протікання металургійних процесів і отримання легованих частинок при розпиленні порошкових електродів

Ключові слова: електродугова металізація, порошковий стержень, легування, газове середовище, розпорошуючий струмінь

Разработана усовершенствованная схема процесса электродуговой металлизации. Она позволяет учесть плавление оболочки и прилегающего порошкового стержня ввиду ограниченного действия распыляющей струи непосредственно на «внутреннюю» поверхность торцов электродов. Этот эффект обеспечивает возможность протекания металлургических процессов и получение легированных частиц при распылении порошковых электродов

Ключевые слова: электродуговая металлизация, порошковый стержень, легирование, газовая среда, распыляющая струя

DEVELOPMENT OF PROPERTIES OF SPRAY FLOW AND NATURE OF PRESSURE DISTRIBUTION IN ELECTRIC ARC METALIZATION

V. Royanov

Doctor of Technical Sciences, Professor*

I. Zakharova

PhD, Associate Professor*

E. Lavrova

PhD, Associate Professor*

E-mail: lavrova.e.v.pstu.edu@gmail.com

*Department of Automation and Mechanization of Welding Production

Priazovskiy State Technical University
Universitetska str., 7, Mariupol, Ukraine, 87500

1. Introduction

Electric arc metallization (EAM) has ample opportunities in comparison with all known methods of metal coating.

The process of electric arc metallization consists in heating the ends of metal electrodes to the melting point by means of an electric arc and then spraying of liquid metal with a compressed air jet.

When a coating layer is applied to the surface of a part, heating of it to 50–70 °C does not cause any structural changes in the metal of the part, i.e. its mechanical properties are preserved, so coating layers can be applied to any materials. Metallization provides a high hardness of the sprayed layer, which increases the service life of the parts restored.

High-quality coatings can be obtained only with strict adherence to the regimes and the technology of the process. Formation of a two-component jet – gas flow and molten particles in the EAM process is of particular importance.

The effect of electrodes on the state of the gas flow and the presence of shocks in the flow around the electrodes consists in a decrease of pressure of the spray jet in the area of the electrodes.

Therefore, the problem of studying the nature of gas pressure distribution in the interelectrode gap, where changes in the gas flow nature occur in the presence of obstacles to the gas flow, becomes urgent. Changes in the gas flow depend on the form of obstacles, flow characteristics. The nature of gas pressure distribution has a strong influence on the formation of anticorrosive, wear-resistant coatings.

2. Literature review and problem statement

An increase in the maximum speed of the air flow improves the quality of metallization when restoring engine crankshafts and other elements, where the metallization process at a distance of more than 120 mm is possible [1]. However, the structure of the air flow during this process is not considered.

To solve the problem of reducing the oxidation potential during electric arc metallization, the spray flux method was used. The presented equipment consists of a steel cylinder, where by means of air supplied to a metal sprayer, a flux solution is dissipated to an average state [2]. The disadvantage of the presented method is the need to use additional equipment and materials (flux solution).

The paper [3] proposes the flow diagram of electric arc metallization with a heterophase flow, an electric arc, a metal sprayer, where thermal dissociation of dissolved substances takes place. However, the presented data do not consider the interaction between the gas flow and obstacles in the form of solids – electrodes located at an angle to the flow.

Data on the state of the gas medium between the ends of the sprayed electrodes at various gaps between them are absent in the literature [4]. Therefore, the study of this factor is important in the analysis of processes of electrode melting with a flux-cored rod.

In the absence of an intense flow, the rod and the sheath of flux-cored wires are melted and actively mixed to produce alloyed particles in the coating [5]. Thus, it seems necessary

to investigate the nature of gas pressure distribution in the interelectrode gap.

Various methods are used for repair and restoration of internal combustion engines, piston-boss bushes, diesel engine sleeves, etc. such as surfacing, spraying, plasma hardening, and also production of parts of special steels.

In the manufacture of many structures, stainless steel and austenitic stainless steel are recommended. These alloys consist of equal amounts of ferrite and austenite in the microstructure. The process of obtaining anticorrosive properties is costly [6]. The manufacture of welded structures of stainless steels is accompanied by a number of difficulties related to weldability [7]. Therefore, the use of stainless steels has a number of restrictions [8].

The restored products undergo various forms of wear and corrosion during operation. Corrosion-resistant coatings can be also applied by surfacing.

The methods of repair and restoration of worn out and damaged components by the surfacing method have been considered [9, 10]. The presented results testify to the need for monitoring and control of outbound processes, coating sizes and strength characteristics.

The manufacture of metal coatings is possible due to a high contact voltage and proximity of contacts between the coating material and the substrate. This results in solid adhesion between the coating and the substrate. The phenomenon of adhesion strength is also present when using electric arc metallization.

The state of the gas medium between the ends of the sprayed electrodes during arc metallization plays an important role in the formation of coatings, so the study of this factor is topical.

3. The aim and objectives of the study

The aim of the paper is to study the state of the gas medium between the ends of the sprayed electrodes and the formation of a spray flow during electric arc metallization. This will increase the strength properties and improve the formation of spray coatings.

To achieve the aim, the following objectives were accomplished:

- to develop methods for studying the effect of electrodes on the air-spray jet characteristics;
- to develop circuits for measuring the total pressure of the spray jet in the interelectrode gap;
- to determine the pressure parameter in the stagnated flow mathematically.

4. Gas flow characteristics during arc metallization

The studies were carried out on stationary spraying pistols EM-17, developed by the All-Russian Research Institute Avtogenmash (Russia) [5]. The material is sprayed by means of an air jet. The working pressure of compressed air is 0.5–0.6 MPa, the flow rate is 60–150 m³ [11, 12]. To form the air-spray jet, spray heads with cylindrical nozzles are used.

Under conditions of electric arc spraying, the pressure of the medium into which the spray gas flows is $P_n=0.1$ MPa. The nozzle-exit pressure is at least 0.2–0.4 MPa being well above the excess pressure $P_a=0.0893$ MPa. The results obtained correspond to drop to the supersonic flow velocity [12].

The flow pattern in the supersonic jet flowing from a plane or axisymmetric nozzle depends on the noncalculability of the jet (1)

$$n = \frac{P_a}{P_n}, \tag{1}$$

where P_a is the nozzle-exit pressure; P_n is the ambient pressure.

It also depends on the nozzle divergence angle, the state of the medium (velocity, density, temperature) where the jet flows, as well as the flow parameters at the nozzle exit (Fig. 1). If $n < 1$, that is, $P_n < P_a$, there are overexpanded flows (1).

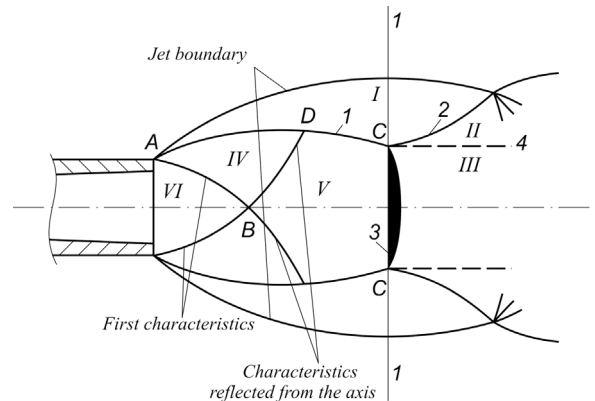


Fig. 1. Supersonic jet flow pattern

The supersonic or noncalculated jet flowing out of the nozzle is conditionally divided into 3 sections (Fig. 1):

- 1 – the initial gas dynamic section, where viscosity and thermal conductivity affect only in a thin boundary layer;
- 2 – the transitional section, where turbulence significantly affects, but there is a constant velocity core, and the maximum velocity along the jet section does not lie on the jet axis;
- 3 – the main section, where the axial velocity becomes maximum over the section.

It is known that the transitional section can be divided into two. The first section – where the constant velocity core is reduced (axial velocity is constant). The second section – where there is no constant velocity core, the axial velocity increases in the direction of the jet, and the maximum velocity along the section does not lie on the jet axis.

In electric arc metallization, axisymmetric (cylindrical) nozzles are used in devices. The flow pattern in the initial section in the case of an axisymmetric supersonic jet with $n > 2$, given in [12], is shown in Fig. 1.

4. 1. Justification of the method for studying the effect of electrodes on the air-spray jet characteristics

The main gas flow characteristics are static and dynamic pressure, gas flow velocity. According to the data of [15], the total pressure is a sufficient characteristic of the gas flow:

$$P_{\Sigma} = P_{st} + P_{dyn}, \tag{2}$$

where P_{st} is the static pressure in the flow; P_{dyn} is the dynamic pressure or velocity head

At any point in the gas flow, the total head can be determined from the equation [19, 20]

$$H = P + \frac{\gamma \omega^2}{2g}, \quad (3)$$

where P is the gas pressure, ω is the flow velocity, γ is the volumetric weight, g is the acceleration of gravity.

Measurement of the gas flow pressure is an essential factor in determining the gas properties and velocity. Depending on whether the gas is at rest or motion, two types of pressure are distinguished. Static (P_{st}) pressure is the internal pressure of a rectilinearly moving gas flow, shown by a manometer, conditionally moving in the direction of the flow. Dynamic pressure (P_{dyn}) or velocity head is the pressure produced by the gas flow due to the energy of its motion.

Static pressure is an important characteristic for measuring the amount of gas by means of resistance to motion and for other purposes. To measure the static pressure of the gas flow, instruments and devices such as a Seurat washer, Niefer device, Rosenmüller device can be used.

When measuring the static pressure (Fig. 2), it is necessary to pay attention to the accuracy of the instrument installation in the flow, since shifts may lead to higher readings of the manometer.

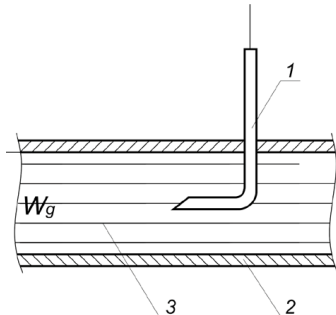


Fig. 2. Total (P_{Σ}) gas flow pressure measuring circuit: 1 – bent tube, 2 – tube walls, 3 – gas flow

In addition, measurement of the static pressure requires the production of an indicator (tube) with side openings (Fig. 3). It is supposed to measure the pressure between the electrode ends, where space is limited by the diameter of electrodes (not more than 3 mm). The manufacture of an indicator tube (hollow needle) with side openings presents considerable difficulties.

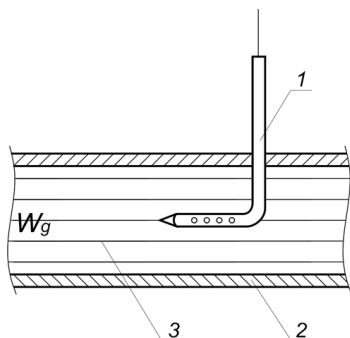


Fig. 3. Static pressure measuring circuit: 1 – indicator, 2 – tube walls, 3 – gas flow

Therefore, the magnitude of the total: static + dynamic pressure was determined in studies using bent medical needles. The accepted circuit for measurements in the interelectrode zone where the electric arc is located is shown in Fig. 4.

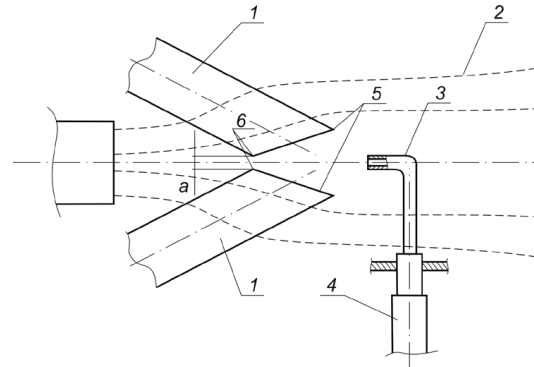


Fig. 4. Circuit of measurements in the spray jet and the interelectrode gap: 1 – models of electrodes, 2 – spray jet, 3 – hollow needle, 4 – retainer, 5 – electrode ends, 6 – interelectrode gap

Such a measuring circuit allows determining the value in different sections of the interelectrode space (center and periphery) and also along the jet. The accepted circuit corresponds to the problem solved in gas dynamics in the flow around a blunt-nosed body and determining the pressure shown by a Pitot tube [12].

The pressure it shows, P_n , corresponds to the pressure in the top of the blunt-nosed body. The ratio of the shock pressure P_1 and the incident flow P is determined by the Rayleigh formula:

$$\frac{P_n}{P_1} = \frac{(K+1)^{\frac{k+1}{k-1}} M_1^2}{2[2(K-1)^{\frac{1}{k-1}} (\frac{2K}{K-1} - \frac{1}{M_1^2})^{\frac{1}{k-1}}]}, \quad (4)$$

where

$$M_1^2 = \frac{V_1^2}{KRT} \quad \text{and} \quad K = \frac{c_p}{c_v}$$

R is the gas constant, ($R=8314 \text{ J/deg}\cdot\text{kmol}$); T_1 is the incident flow temperature.

If to substitute P_1 with the pressure of the adiabatic flow, we obtain a formula for determining the ratio of the pressure in the stagnated flow and the Pitot tube readings behind the flow.

$$\frac{P_n}{P_1} = M \frac{2K}{K-1} \left(\frac{1 - \frac{K-1}{K+1} M_1^2}{M_1^2 - \frac{K-1}{K+1}} \right)^{\frac{1}{k-1}} = \left(\frac{V_1}{V_2} \right)^{\frac{1}{k-1}} = e^{-\frac{\Delta S}{R}}. \quad (5)$$

The formula shows that the deceleration pressure behind the shock is less than in front of it.

Due to the fact that in arc metallization, cylindrical nozzles operate in the underexpanded mode, this mode is referred to as non-calculated. In the supersonic jet of the non-calculated regime, there are shocks accompanied by shock waves. There is the possibility of a visual examination of the effect of electrodes on the structure and shape of the jet and individual sections, on the jet length variation, using shadow photography.

For these purposes, an installation, allowing to record the gas spectrogram of the jet on a film and to determine the influence of electrodes on structural changes has been developed.

4. 2. Experimental research on the effect of electrodes on the spray jet properties

Based on the previously proven method, the installation to measure the total pressure in the spray jet (Fig. 5), which allows modeling the arrangement of electrodes in the flow was developed. The installation consists of the spraying system of the arc spraying pistol with a cylindrical nozzle, a holder of electrodes at different angles to each other, a working body (indicator). The indicator is a hollow needle with a bent end at an angle of 90° and verticals (Fig. 5). The needle hole diameter is 0.20 mm. The needle channel is connected to a manometer with a scale of 0.1...0.9 MPa and scale interval of 0.005 MPa, which allowed determining the pressure value and degree of rarefaction (vacuum) in the area between the electrode ends.



Fig. 5. Scheme and appearance of the working part of the installation for determining P_{Σ}

The installation has a device for displacing the needle along and across the electrode ends. In the experiment, the electrodes were installed at an angle of 30–35° under industrial standards by metal spraying pistols EM-17. The bevel angle of the electrode ends was modeled taking into account high-speed filming, the nature of the electrode generation after the arc stopped functioning.

Based on the analysis of the influence of various factors on the results of measurements (air pressure fluctuations in the network, humidity, air temperature at different times of the day, etc.), the volume of the population of experiments was $N=10...15$. Based on the results of the experiments, the arithmetic mean was determined

$$\bar{X} = \sum_{i=1}^n x_i \frac{m_i}{n}, \tag{6}$$

where m_i is the number of close i -th results; n is the number of observations; x_i are the values obtained.

It should be noted that deviations during measurements do not exceed 3...5 %. In the course of the experiment, we determined the total pressure variation along the spray jet without the sprayed electrodes and with the electrodes at different values of the gap between the ends. The curves of pressure variation (Fig. 6) along the spray jet show that with increasing distance to the nozzle exit section, the pressure decreases and reaches the value equal to atmospheric (Fig. 6).

When the pressure at the spraying system inlet of the metal spraying pistol is changed, the above atmospheric pressure in the spray jet remains at a distance to the nozzle exit section of 30 mm or more, a sharper decrease (jump) in the total pressure is not observed. At high pressures, a pressure ripple occurs, corresponding to shock waves.

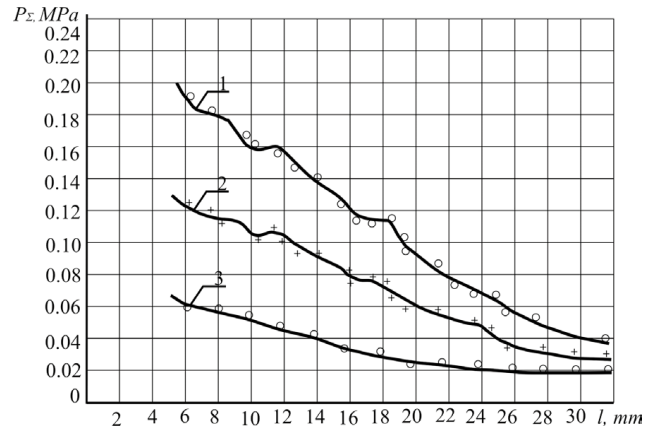


Fig. 6. Variation along the spray jet (without electrodes) at different pressures at the spraying system inlet: 1 – inlet pressure 0.55 MPa; 2 – inlet pressure 0.3 MPa; 3 – inlet pressure 0.1 MPa

The graphs (Fig. 6, 7) show the results of measuring the total pressure in the area between the electrode ends at different levels from the nozzle axis and the spray jet behind the electrodes. The diameter of the electrodes is 2.4 mm, corresponding to the minimum diameter of the flux-cored wires manufactured by an industrial method, the bevel angle of the ends is 30°, the spraying system inlet pressure is 0.5 ± 0.05 MPa. The spray nozzle diameter is 3.0 mm.

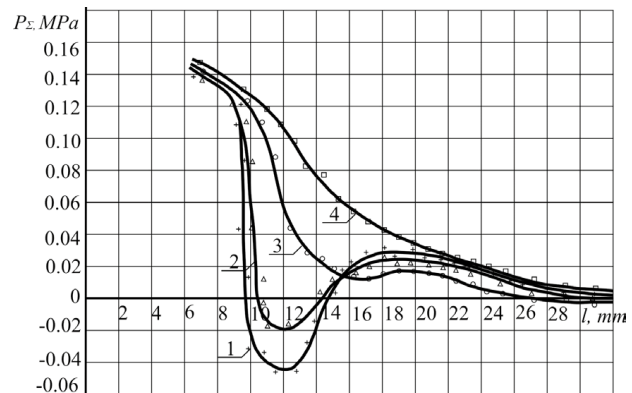


Fig. 7. Distribution in the interelectrode gap, depending on the gap size (along the nozzle axis): 1 – 0.2 mm gap; 2 – 0.5 mm gap; 3 – 1 mm gap; 4 – 2 mm gap

The presented research results show:

- the presence of the electrodes affects the uniformity of distribution of the total pressure of the spray jet in the area of the electrodes. Between the electrode ends, the total (static and dynamic) pressure decreases;
- the drop in the total gas pressure between the electrodes depends on the gap size. Its value is inversely proportional to the distance between the inner electrode ends. With a gap size of up to 0.5 mm, the minimum value is below atmospheric (Fig. 7), and with a 1 mm gap – close to atmospheric ≈ 0.018 MPa. With a 2 mm gap, the pressure drop in the interelectrode gap is practically not observed in Fig. 7;
- in the absence of an interelectrode gap, rarefaction is created, the value of which (under the experimental conditions) reaches ≈ 0.044 MPa;
- when the measurement points are shifted from the center of the electrode ends (from the nozzle axis) “vertically”

to the periphery, the pressure increase is observed, both in the absence and in the presence of a gap. In the absence of a gap, within the electrode ends, pressure varies from the center to the outer part of the electrode ends in the range of 0.044...0.038 MPa. With the gap increase, the pressure in the interelectrode gap periphery is close to atmospheric (Fig. 7) and accordingly equal to (under the experimental conditions) $P_z = 0,16$ MPa with a gap between the inner electrode ends of 1.4 mm.

- the length of the pressure drop (rarefaction) zone does not exceed the length of the electrode ends;

- the pressure in the interelectrode gap depends on the air pressure variation at the spraying system inlet. As the pressure P_{inlet} decreases, the value of rarefaction in the interelectrode gap decreases and pressure increases, the difference with the nozzle outlet pressure decreases, which is probably connected with the approach of the flow to laminar.

The results of the research are confirmed by the gas spectrograms obtained by means of shadow photography of the jet in the zone of the electrode ends. The shooting was conducted in two mutually perpendicular directions: from the side surface of the electrodes (Fig. 8, *a*) and from “above the electrodes” (Fig. 8, *b*).

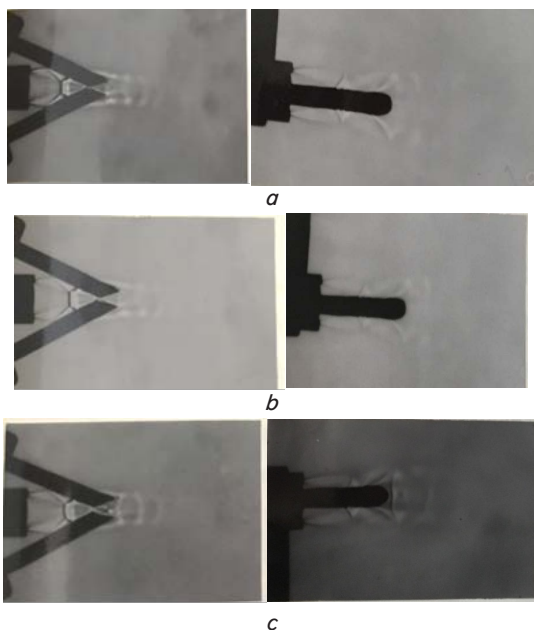


Fig. 8. Effect of electrodes on the spray jet structure (gas spectrograms): *a* – without a gap; *b* – 0.5 mm gap; *c* – 1.2 mm gap

The gas spectrograms show that the electrodes are located in the zone of the secondary expansion of the jet in the region limited by the first shock waves. This leads to a flow of rarefaction and “deformation” of the second section of the spray jet at a gap size of 0 to 2 mm, (Fig. 8, *c*). With gaps from 0 to 1 mm, there is no Mach disc at the end of the second segment. The shock zones of the flow in the interelectrode gap are not observed. At the initial section of the jet, the zones are clearly pronounced. In the subsequent section, these zones are difficult to distinguish at gaps of 0, 0.5 mm. The contours of these zones begin to recover at a gap of 1.2 mm. With a 1.2 mm gap (Fig. 8, *a*), the degree of flow separation is reduced, the jet penetrates between the electrode ends, and at the end of the second segment, a Mach disk is

formed. On the “side” views, with a gap value of 0 to 0.5 mm, jet separation is clear during the flow around the electrodes, the formation of the jet sections behind the electrodes is not observed. Jet formation is observed in the zone behind the electrodes with a gap of 1.2 mm.

Thus, the above gas spectrographs show that the presence of electrodes affects the spray jet structure, there is a flow separation during the flow around the electrodes, the electrode ends are located in the zone of rarefaction.

4. 3. Research on the effect of the spray jet on the formation of an arc discharge and the flow of particles of the sprayed electrodes

According to the above, direct pressure measurement and shadow photography show that the presence of electrodes affects the total pressure distribution in the interelectrode space and along the spray jet. At the same time, melting of electrodes during electric arc spraying is carried out under the influence of arc discharge heat. It is known that the arc is divided into two “tongues”, from which the flow of particles is separated. At the same time, a number of researchers considered the arc discharge to be a quasi-solid impermeable body [4–7].

In order to study the interaction between the electric arc and the gas flow, in shadow photography of the gas jet, the arc discharge was simulated by means of solid and plastic inserts – simulators fixed in the interelectrode gap. Shadowgraphs are shown in Fig. 9. The presence of the solid simulator in the interelectrode gap (in the form of a 2 mm ball) leads to the presence of a pronounced flow around the electrodes at all values of the gap between the electrodes from 0 to 2 mm. The results correspond to the gas spectrograms obtained earlier (photography of the jet without simulators) in the absence of a gap between the electrodes (Fig. 9, *a*).

The degree of deformation (elongation) depends on the size of the gap between the electrodes. With the gap increase, deformation of the flexible simulator increases and reaches the maximum values with a gap of more than 3 mm. With a gap between the electrodes of 0...1 mm, the gas jet has almost no effect on the simulator and its position is similar to the initial one (Fig. 9, *d, e*) (without the gas jet effect).

With a 2...3 mm gap, considerable deformation of the flexible simulator is observed, which is shown on photographs “in the plane of the electrodes and the spray nozzle” and when photographing the electrodes “from the side” (Fig. 9, *c*). At a 2 mm gap, the opening angle of the gas flow decreases, and the shape of the jet approaches that recorded during photographing without simulators in the interelectrode gap with 2 mm gaps.

The experiments show that in the presence of the solid simulator in the interelectrode gap, there is a stable flow separation between the electrodes and the simulator with gaps from 0 to 2 mm.

In the presence of the flexible simulator, which probably corresponds more to the real arc discharge, the flow separation during the flow around takes place at gaps from 0 to 1 mm. With gaps greater than 1 mm, the flow penetrates into the interelectrode gap, actively affects the simulators and causes considerable deformations. This takes place in real conditions and leads to the arc deformation (or breaking) at large (more than 1 mm) gaps between the electrodes. In order to determine the influence of the gas jet separation on the formation of the arc discharge and particles of the sprayed electrodes, photography of the interelectrode zone

and the arc from the side of the electrodes was carried out. The combination of light filters was used: orange + light green, exposure 0.002...0.008 sec. The resulting photographs (Fig. 10, 11) show that the shape of the arc discharge from the “side” view is close to the shape of the spray jet during the flow around the electrode ends.

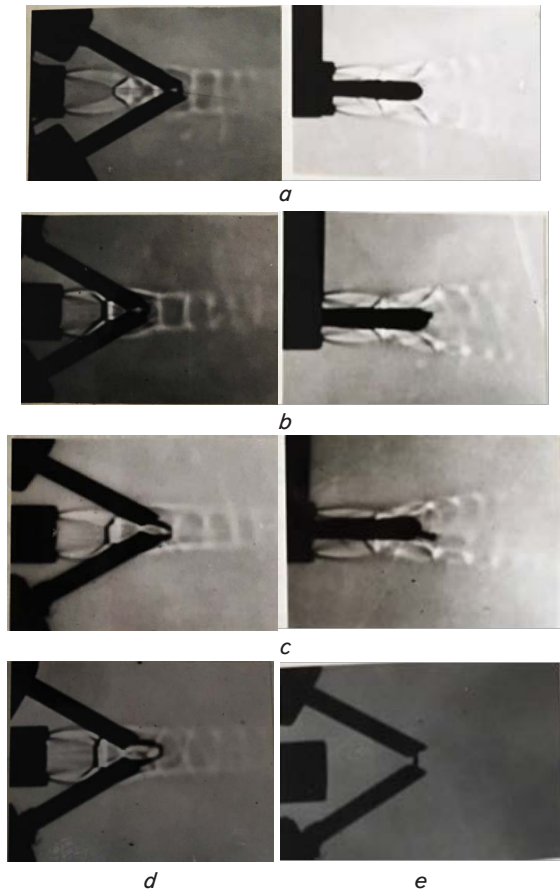


Fig. 9. Interaction between the elastic arc simulator and the spray gas jet (gas spectrograms): *a* – 0 mm gap, weak arc intensity; *b* – 1 mm gap, more pronounced areas of discharge in the arc flow behind the electrodes; *c* – 2 mm gap, arc flow gain; *d* – 3 mm gap, view “from above”; *e* – 3 mm gap, without a jet



Fig. 10. Arc discharge and particle flows of the sprayed flux-cored electrodes

In the center, the luminescence region is smaller than in the periphery, which is probably due to the jet discontinuity and pressure drop in the center, Fig. 11. At the same time, the researchers shoot, as a rule, “from above the electrodes and the

nozzle” and record the arc elongation, considering that this is due to its deformation by the gas flow. The presented photographs (Fig. 10, 11) allow us to state that the arc discharge is located in the zone of low pressure (interelectrode space) and, due to thermal action, causes active luminescence of the gas gap separated by the electrodes.



Fig. 11. Arc discharge and particle flows of the sprayed flux-cored electrodes with pressure drop in the center

The photographs (Fig. 10, 11) show that the particles located at the electrode ends form two flows according to the shape of the spray gas jet obtained by means of shadow photography. Separation occurs when the solid and flux-cored electrodes are sprayed. Photography from above the electrodes and the nozzle, used earlier by the researchers, did not allow observing the transfer and formation of particles along the outer parts of the electrodes, which takes place in real conditions.

5. Results of the research on sources with forward and bridge converters

In order to confirm the proposed refined flow diagram of electric arc spraying, filming of melting of the flux-cored rod was carried out, and the study of melting of the sheath without the rod and 06H18N9T alloyed wire was also conducted for comparison. Filming was made by the SKS-1 camera at a speed of 2,450 frames/sec (after acceleration) on the KN-2 black and white film.

The backlighting was carried out with the NF 7000-01.78 NARVA mercury lamp using the mirror-reflecting and focusing system. When shooting, the electrodes were located in a vertical plane: the anode – above, the cathode – below. The arc was powered by the VDU-505 rectifier using a stiffness characteristic. Optimum metallization parameters under the flow diagram are given in Table 1.

Table 1

Arc metallization parameters during high-speed filming

No.	Sprayed material	Arc metallization parameters				Distance between the arc and the nozzle exit section	Note
		I_a , A	U_a , A	P_{airs} , MPa	V_{feed} , m/s		
1	Flux-cored wire	260	35	0.55	3.1	20	Diameter 2.4
2	Sheath	220–230	31–33	0.55	3.1	20	Without flux-cored rod
3	Solid wire	180	32	0.55	3.4	20	Diameter 2.0

The resulting film material was processed. Viewing of films and analysis of records were carried out. The nature of melting of flux-cored wires and solid wires shows no significant differences. When melting the flux-cored wire on the anode end surface, liquid metal is stretched and formed as a thread of considerable length, which is typical of solid wires, according to the literature [9]. On the cathode end surface, in contrast to solid electrodes, particles of a spherical shape are periodically formed along with the particles of an elongated shape. It should also be taken into account that the flux-cored rod is not electrically conductive. The influence of the presence of furnace charge on the melting nature of flux-cored wires is confirmed by the melting nature of the sheath. The record (Fig. 12) shows that the melting nature of the sheath is close to melting of solid wires. The process of formation and separation of particles at the cathode and the anode of the tubular electrode is the same as for solid wires. However, the dispersion of the particles is somewhat higher, which is probably due to an increased current density and a more efficient use of arc heat for the sheath melting (no rod). In all the analyzed cases of the electrode material melting, the arc is placed between the slanted outer electrode ends, as if in a “funnel”.

It was also found that when melting flux-cored wires, melting of the rod and the sheath occurs simultaneously. Separation and transport of the sheath particles and furnace charge components are not observed. This is probably due to the fact that in arc metallization with flux-cored wires, the near-electrode regions are located on the inner parts of the ends of the metal sheath of the sprayed electrodes. As a result, the arc has an active impact on the rod of the flux-cored electrode. Melting of the rod components and blending with the sheath when liquid metal moves from the “inner” part of the electrode ends to the outer peripheral parts are provided. The results of the research suggest the following process flow diagram of melting flux-cored wires (Fig. 12).

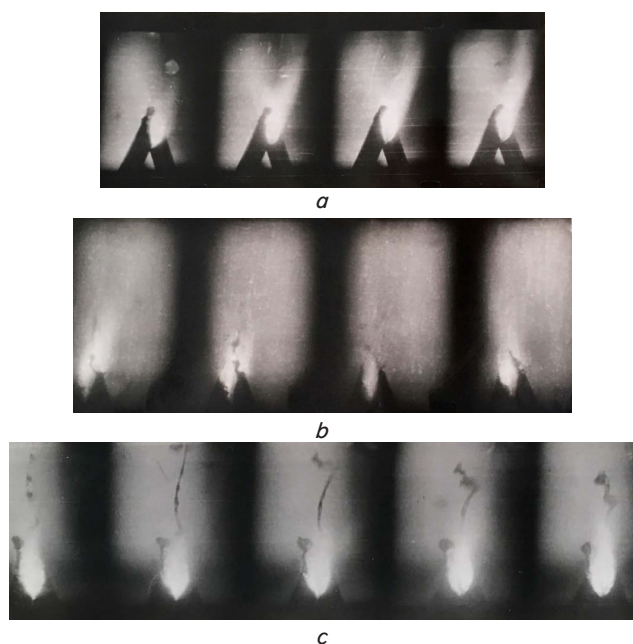


Fig. 12. Records of melting of various types of electrodes during arc metallization: *a* – 06H18N9T wire, *b* – 08KP tubular electrode, *c* – PP-MM-2 flux-cored wire

In view of the limited effect of the spray jet directly on the “inner” surface of the electrode ends, melting of the sheath and the adjacent flux-cored rod first occurs. In the process of accumulation, liquid metal moves to the periphery of the electrode ends under the influence of electrodynamic forces, which provides blending and interaction between the sheath metal and the flux-cored rod. On the periphery of the electrode ends, there is a separation and transfer of the particles of the sprayed electrodes under the action of the spray jet. This ensures the possibility of metallurgical processes and production of alloyed particles when spraying flux-cored electrodes.

6. Discussion of the results of adjustment of the process flow diagram of electric arc metallization

The above results of direct measurements confirmed the presence of pressure drop in the interelectrode space.

The influence of the electrodes on the formation of the arc discharge and particle flows of the spray jet, as well as the absence of direct influence of the gas flow on the “inner” parts of the electrode ends are established.

The obtained experimental data allow introducing refinements into the process flow diagram of electric arc metallization (Fig. 13).

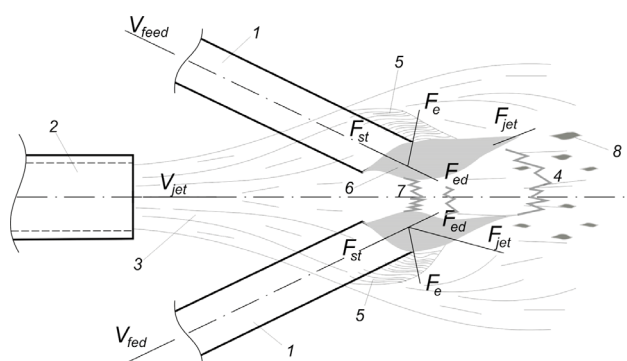


Fig. 13. Refined flow diagram of electric arc spraying: 1 – sprayed electrodes; 2 – air nozzle; 3 – spray air jet; 4 – electric arc; 5 – vortex (rarefaction) area; 6 – liquid metal at electrode ends; 7 – interelectrode gap; 8 – sprayed metal particles; F_{st} – surface tension force; F_{ed} – electrodynamic force; F_{jet} – force of the gas jet impact on liquid metal; F_e – force of the vortex (rarefaction) impact in the flow of the gas jet around the electrodes

The presented flow diagram (Fig. 13), along with the known elements, considers the presence of a drop in the area of the electrode ends, as well as the air flow around the electrodes and its influence on the shape and transport of particles.

The above results make it possible to assert that, with a stable arc metallization process, arcing occurs under conditions where the pressure of the gas medium between the electrodes is close to atmospheric. Physical conditions for the formation of liquid metal at the electrode ends are close to the formation of droplets during consumable electrode arc welding.

It is known that the following forces act on liquid metal: P_{st} – surface tension force that holds liquid metal at the

electrode ends; P_{ed} – electrodynamic force (pinch effect); P_{jet} – force of air spray jet impact on liquid metal along the jet, which facilitates the removal of droplets from the electrode ends.

The advantages of the research in comparison with analogs is the consideration of the forces acting on liquid metal – vortex force (P_v). This force arises in the air flow around solid cylinders of electrodes and promotes liquid metal separation due to rarefaction. Taking into account the above forces, the condition of liquid metal retention at the electrode end will be:

$$P_{st} \geq \overline{P_{jet}} + \overline{P_{ed}} + \overline{P_y}. \quad (7)$$

The condition of liquid metal separation from the electrode ends

$$P_{st} \leq \overline{P_{jet}} + \overline{P_{ed}} + \overline{P_y}. \quad (8)$$

In the absence of the gas flow, the condition of liquid metal retention at the electrode end will be the condition of liquid metal balance at the electrode ends: $\overline{P_{st}} \leq \overline{P_{ed}}$, that is, metal separation from the electrode ends is due to the forces of the air spray jet. In the absence of the jet, metal is held by the surface tension force. Thus, there may be some time to find liquid metal in the absence of the gas flow and limited by the action of air oxygen. Then, under the impact of the flow, liquid metal is actively removed from the electrode ends under the action of the above forces. This principle underlies the process of electric arc spraying with a pulsating feed of the air-spray jet.

The development of the presented research may consist in the design of additional structural elements (pulsing nozzles) for the formation of an air jet during electric arc metallization.

7. Conclusions

1. The process flow diagram of electric arc metallization is developed taking into account the influence of the vortex

force, which allows modeling various positions of the electrodes in the spray jet. Direct measurements of the total (static + dynamic) pressure in the local zone between the electrode ends used for arc metallization are made.

2. The results of direct measurement of the gas pressure in the interelectrode gap (when modeling the interaction between the electrodes and the spray flow) have confirmed the presence of pressure drop in the spray jet in the region of the sprayed electrodes. The results of the research have allowed clarifying the nature of pressure distribution in the interelectrode gap.

3. It was found that for models of electrodes with a diameter of 2.4 mm with a gas pressure at the spraying system inlet of the arc spraying pistol $P_{inlet}=0.5\pm 0.05$ MPa and the absence of a gap between the inner parts of the electrode ends, rarefaction is created in the center of the interelectrode gap – 0.044 MPa. With the gap increase, the degree of pressure drop decreases: when the gap varies from 0 to 1.0 mm, the pressure in the center between the electrode ends varies within 0.044...0.16 MPa. With a gap between the electrode ends of 2 mm or more, the pressure drop is negligible. The characteristic changes in the spray jet structure in the presence of electrodes are confirmed by the results of shadow photography.

4. The presented research results allowed making adjustments to the process flow diagram of electric arc metallization. The presence of the zone of air flow around the electrodes and the pressure drop in the interelectrode gap are taken into account. Optimum conditions for the arc functioning are achieved with such a ratio of the rates of feeding and melting of the electrodes, when the gap between the inner surfaces of the ends is within 0.5...1.0 mm.

5. The results providing a stable process of electric arc metallization are obtained. When using 2...2.4 mm electrode wires, arcing occurs in the absence of direct action of the spray jet on the inner parts of the electrode ends. The pressure between the electrodes is close to atmospheric and the physical conditions for the formation of liquid metal at the electrode ends are close to the formation of droplets during consumable electrode arc welding.

References

1. Litovchenko, N. N. Ways of improving equipment and technology of electric arc metallization [Text] / N. N. Litovchenko, V. N. Logachev // Tractors and agricultural machinery. – 2013. – Issue 11. – P. 52–54.
2. Vorobiev, P. A. Method of aerosol fluxing in electric arc metallization [Text] / P. A. Vorobiev, M. Y. Yusim, N. N. Litovchenko, V. I. Denisov // Method of aerosol fluxing in electric arc metallization. Proceedings of GOSNITI. – 2008. – Issue 101. – P. 201–204.
3. Litovchenko, N. N. Influence of the flow rate of heterophase flux on the physico-mechanical properties of the electrometallic flow [Text] / N. N. Litovchenko, B. I. Petryakov, A. A. Tolkachev, S. A. Blokhin // Welding production. – 2013. – Issue 6. – P. 43–47.
4. Solov'ev, R. Yu. Metal-carbothermal methods of reducing the degree of oxidation of dispersed metal in electric arc metallizing [Text] / R. Yu. Solov'ev, P. A. Vorob'ev, N. N. Litovchenko // Welding International. – 2013. – Vol. 27, Issue 5. – P. 423–427. doi: 10.1080/09507116.2012.715930
5. Denisov, V. I. Activation of the process of electric arc metallization with liquid hydrocarbon fuel [Text] / V. I. Denisov, N. N. Litovchenko, V. N. Logachev, A. A. Tolkachev // Proceedings of GOSNITI. – 2015. – Issue 12. – P. 160–165.
6. Lo, K. H. Recent developments in stainless steels [Text] / K. H. Lo, C. H. Shek, J. K. L. Lai // Materials Science and Engineering: R: Reports. – 2009. – Vol. 65, Issue 4-6. – P. 39–104. doi: 10.1016/j.mser.2009.03.001
7. Olsson, J. Duplex – A new generation of stainless steels for desalination plants [Text] / J. Olsson, M. Snis // Desalination. – 2007. – Vol. 205, Issue 1-3. – P. 104–113. doi: 10.1016/j.desal.2006.02.051
8. Charles, J. Duplex stainless steels – a review [Text] / J. Charles // In: Proceedings of 7th International conference on DSS. – 2007. – P. 35–42.
9. Voutchkov, I. An integrated approach to friction surfacing process optimization [Text] / I. Voutchkov, B. Jaworski, V. I. Vitanov, G. M. Bedford // Surface and Coatings Technology. – 2001. – Vol. 141, Issue 1. – P. 26–33. doi: 10.1016/s0257-8972(01)01127-6

10. Yamashita, Y. Newly Developed Repairs on Welded Area of LWR Stainless Steel by Friction Surfacing [Text] / Y. Yamashita, K. Fujita // Journal of Nuclear Science and Technology. – 2001. – Vol. 38, Issue 10. – P. 869–900. doi: 10.1080/18811248.2001.9715112
11. Ivanov, V. Improving the Efficiency of Strip Cladding by the Control of Electrode Metal Transfer [Text] / V. Ivanov, E. Lavrova // Applied Mechanics and Materials. – 2014. – Vol. 682. – P. 266–269. doi: 10.4028/www.scientific.net/amm.682.266
12. Royanov, V. A. Equipment for electric arc metallizing with pulsed discharge of the air-spraying jet [Text] / V. A. Royanov, V. I. Bovikov // Welding International. – 2015. – Vol. 30, Issue 4. – P. 315–318. doi: 10.1080/01431161.2015.1058006

У роботі виконано дослідження закономірностей зв'язку флуктуацій числа і розмірів зважених у рідині часток на характеристики поля об'ємних ультразвукових хвиль. Виявлено, що величина згасання об'ємних ультразвукових коливань високої частоти (≥ 5 МГц) у реальній пульні залежить практично тільки від концентрації твердої фази і крупності часток подрібненого матеріалу

Ключові слова: газові бульбашки, збагачення руди, об'ємні ультразвукові хвилі, розподіл часток, характеристики пульни

В работе выполнено исследование закономерностей связи флуктуаций числа и размеров взвешенных в жидкости частиц на характеристики поля объемных ультразвуковых волн. Обнаружено, что величина затухания объемных ультразвуковых колебаний высокой частоты (≥ 5 МГц) в реальной пульне зависит практически только от концентрации твердой фазы и крупности частиц измельченного материала

Ключевые слова: газовые пузырьки, обогащение руды, объемные ультразвуковые волны, распределение частиц, характеристики пульпы

UDC 621.926:34.16

DOI: 10.15587/1729-4061.2017.118943

INVESTIGATION OF THE EFFECT OF CHARACTERISTICS OF GAS-CONTAINING SUSPENSIONS ON THE PARAMETERS OF THE PROCESS OF ULTRASONIC WAVE PROPAGATION

V. Morkun

Doctor of Technical Sciences,
Professor, Vice-Rector for Research**
E-mail: morkunv@gmail.com

N. Morkun

Doctor of Technical Sciences,
Associate Professor, Head of Department*
E-mail: nmorkun@gmail.com

V. Tron

PhD, Associate Professor*
E-mail: vtron@ukr.net

S. Hryshchenko

PhD, Head of Section
Section of scientific and technical information**
E-mail: s-grischenko@ukr.net

*Department of automation,
computer science and technology**

**Kryvyi Rih National University

Vitaliya Matushevycha str., 11, Kryvyi Rih, Ukraine, 50027

1. Introduction

Ultrasonic methods and technologies are widely used at present in various research projects. Specifically, they are applied when examining, identifying, and controlling quality of different materials [1]. For example, in order to distinguish characteristics of the varieties of enriched ore raw materials [2–4].

To optimize control over processes of enrichment mineral resources, an important aspect is the availability of qualitative information on the characteristics of technological media [5]. A need to exercise operational control over characteristics of the solid phase of the pulp is also stressed by the existence of uncertainty in the parameters of technological

units [6]. It should be noted that the application of ultrasonic methods in a given case would provide the required performance speed and measurement accuracy.

Significant losses of the useful component in wastes of enrichment production lead not only to a decrease in performance indicators, but also negatively affect the environment [7, 8]. One of the ways to reduce the negative impact of the loss of a useful component is to improve efficiency of flotation processes. Paper [9] proposed a method for ultrasonic treatment of particles of the enriched ore materials in order to better clean grains of the useful component from the gangue. A positive effect is also noted of ultrasonic oscillations on the formation of gas bubbles and maintaining a cavitation regime, which also improves efficiency of flotation [10, 11].